Materials Research Proceedings 41 (2024) 60-69 https://doi.org/10.21741/9781644903131-7

On the scalability of strength and presumed size effects in SLM-produced 316L stainless steel

VYSOCHINSKIY Dmitry[1,a*], MOE Ole-Bjørn[2]

[1] Jon Lilletuns vei 9, 4879, Grimstad, University of Agder, Norway

[2] Jon Lilletuns vei 9, 4879, Grimstad, Mechatronics Innovation Lab, Norway

[a]dmitry.vysochinskiy@uia.no

Keywords: Powder Bed Fusion, Selective Laser Melting, 316L, Metal Additive Manufacturing, Mechanical Properties, L-PBF

Abstract. As additive manufacturing (AM) technology advances toward the production of structurally utilized metallic components, an accurate evaluation of mechanical properties becomes crucial. Understanding the effect of the printed cross-section size on material strength is exceptionally important since AM technology, especially laser powder bed fusion (L-PBF), enables topology optimization and favors the production of thin struts, lattice structures, and other small cross-sections, as well as thin-walled profiles. Structural designers need to know to what degree the size of the printed cross-section might affect material strength. This study focuses on the effect of printed cross-section size on the mechanical properties of L-PBF-produced 316L stainless steel. The findings reported in existing literature so far are conflicting, indicating a need for further investigation. In the presented paper, the mechanical properties of net-shape printed samples with cross-section diameters ranging from 2.5 mm to 6.0 mm are compared. Tensile tests reveal that smaller diameter net-shape samples exhibit lower strength compared to larger diameters. Machined samples display higher strength than net-shape samples. The observed size-dependent strength variations in L-PBF-produced 316L stainless steel can be explained by the surface layer being weaker than the core of the sample. Whether the effect is due to differences in microstructure between the surface and core of the sample or is simply caused by a reduction of the effective cross-sectional area due to surface roughness could be debated, but both factors are likely to contribute to the phenomenon.

Introduction

As additive manufacturing technology progresses beyond modeling and rapid prototyping towards the production of structurally utilized parts, challenges related to the accurate evaluation of mechanical properties of AM-produced materials become more pronounced. When it comes to additive manufacturing of metallic materials, two common techniques allowing the production of essentially fully dense parts are Directed Energy Deposition (DED) and Powder Bed Fusion (PBF) using standard terminology [1]. The designation Laser-Powder Bed Fusion (L-PBF) is also commonly applied to distinguish processes where a laser is used as a power source, such as Selective Laser Melting (SLM) and Selective Laser Sintering (SLS), from processes where an electron beam is used as a power source, designated as Electron Beam Powder Bed Fusion (EBPBF). While DED has a melt pool is about 0.5-1.0 mm in diameter [2], the typical melt pool size for L-PBF is about 0.2-0.4 mm [3], allowing the printing of fine geometrical details and favoring the use of thin-walled and lattice structures to save weight. This underscores the importance of comprehending the effects of cross-section size on the mechanical properties of the produced printed material, especially in L-PBF processes.

Another issue tied to understanding the effect of printed cross-section size on mechanical properties is the need to comprehend how the rough surface produced by the L-PBF process affects

the mechanical properties of the material. This is more critical for L-PBF processes where the rough surface is commonly retained, as opposed to DED processes where the rough surface is usually machined away in post-processing to meet surface quality and dimensional tolerance requirements. In L-PBF, two different laser scanning patterns are often used on the surface and in the middle of the cross-section, with a hatching pattern used in the bulk and a contour scanning used on the surface to improve surface quality. This is likely to result in differences in microstructure and mechanical properties between the surface and bulk material. Understanding these effects is essential for structural designers to determine when the inhomogeneous cross-section needs to be considered and when it is safe to treat the cross-section as homogeneous.

When it comes to SLM-produced 316L stainless steel, the material this article focuses on, there are studies that report strength to decrease with cross-section size, studies that report no difference in strength for different cross sections sizes and studies that report strength to increase with cross-section size. An example of a study that reports higher strength and ductility for smaller cross-section samples is study by Yu et al. where initial result were published in [4] and expanded study was published in [5]. The authors attribute the effect to finer grain structure of the surface layers [4], [5]. An example of study that finds no difference in strength for different diameters is study by Bültmann et al. [6] who reported the tensile and yield strength of 0.3 mm to 0.7 mm SLM-produced 316L micro-struts to be virtually independent of the strut diameter but lower than the strength of a larger diameter machined SLM-produced sample. There are several examples of studies that report lower strength for smaller cross-section size such as the study by Wang et al. [7] who tested struts of 0.25 mm to 2.0 mm diameter and observed increase in strength with the sample diameter and study by Roach et al. [8] who tested samples with square cross-section with dimensions from 0.4 mm up to 6.25 mm [8].

Thus, the results in the literature are contradictory, and more experimental evidence needs to be gathered in order to justify and understand the effect of printed cross-section size on the strength of SLM-produced 316L stainless steel in a systematic manner. In the presented paper, we compare the strength of SLM produced samples in the diameter range from 2.5 mm to 6.0 mm to quantify the effect of cross-section size on strength. We also compare machined samples with net-shape produced samples of the same diameter to observe the difference and justify the effect of the surface layer on strength.

Materials and Methods

The tensile samples were designed for use with a 25 mm gauge length extensometer, with a total of 4 sets of 4 samples produced. The sample geometry is illustrated in Fig. 1. The machined samples were cut from 10 mm diameter printed cylinders using a lathe machine. Fig. 1 schematically shows the printed cylinder outline and the final sample geometry. The net-shape samples were tested as printed, meaning the required sample geometry was achieved through 3D printing without any additional machining. The raw material used for printing was PowderRange gas-atomized 316L stainless steel alloy powder designed for L-PBF, with a particle diameter range of 15-53 μm.

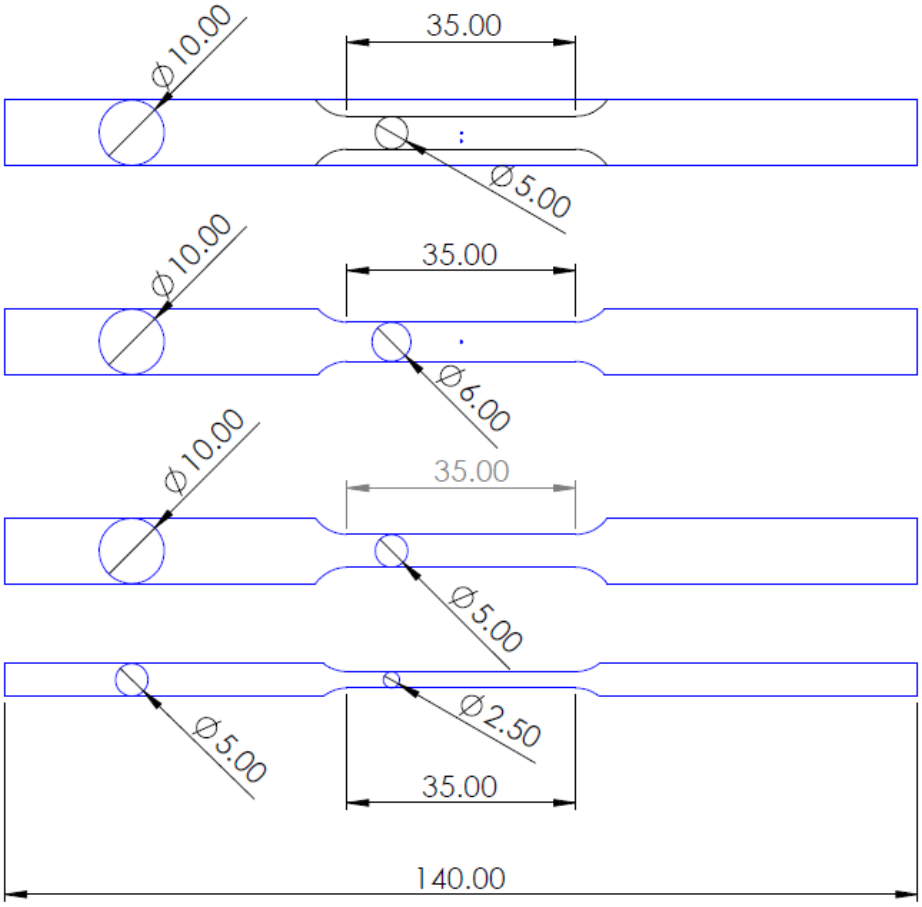

Figure 1. Dog-bone samples geometry: machined, d=6.0 mm, d=5.0 mm and d=2.5 mm.

The samples were printed on a 48 *mm* x 48 *mm* build plate using the SLM®280 metal printer. As Fig. 2 indicates, all samples were oriented vertically i.e. only vertical direction (also commonly called build direction) was tested. The vertical direction was chosen as SLM-produced metals are anisotropic, and the samples oriented in the vertical direction usually display lower strength, although there might be exceptions as shown by Hitzler et al. [9]. The printing layer thickness was set to 60 µm and argon gas was used as protective atmosphere. Build chamber temperature was 100 degrees centigrade and the substrate temperature was ambient. Different combinations of laser power and scanning speed were applied to different parts of the print, but the ones that were used to construct gauge section of the samples were 150 W laser power combined with 350 mm/s scanning speed for contour scanning and 350 W laser power combined with 950 mm/s scanning speed for hatching as Fig. 2 indicates.

The tensile tests were performed using 25 kN SI-plan tension machine with hydraulic grips. The machine is equipped with load cell, build-in position sensor and clip-on LVDT-based extensometer with gauge length of 25 mm. The target strain rate was 0.00025 s^{-1}, which is "Range 2, recommended rate unless otherwise specified" in accordance to the testing standard [10]. The specimen parallel length was 35 *mm*, thus the target strain rate was achieved by setting crosshead separating rate to 0.00875 *mm/s*. The elongation at fracture %EL was measured manually by applying markings on the specimen spaced $l_0=5d_0$ and using a caliper with 0.05 mm accuracy, plastic area reduction %RA was also measured using the same caliper.

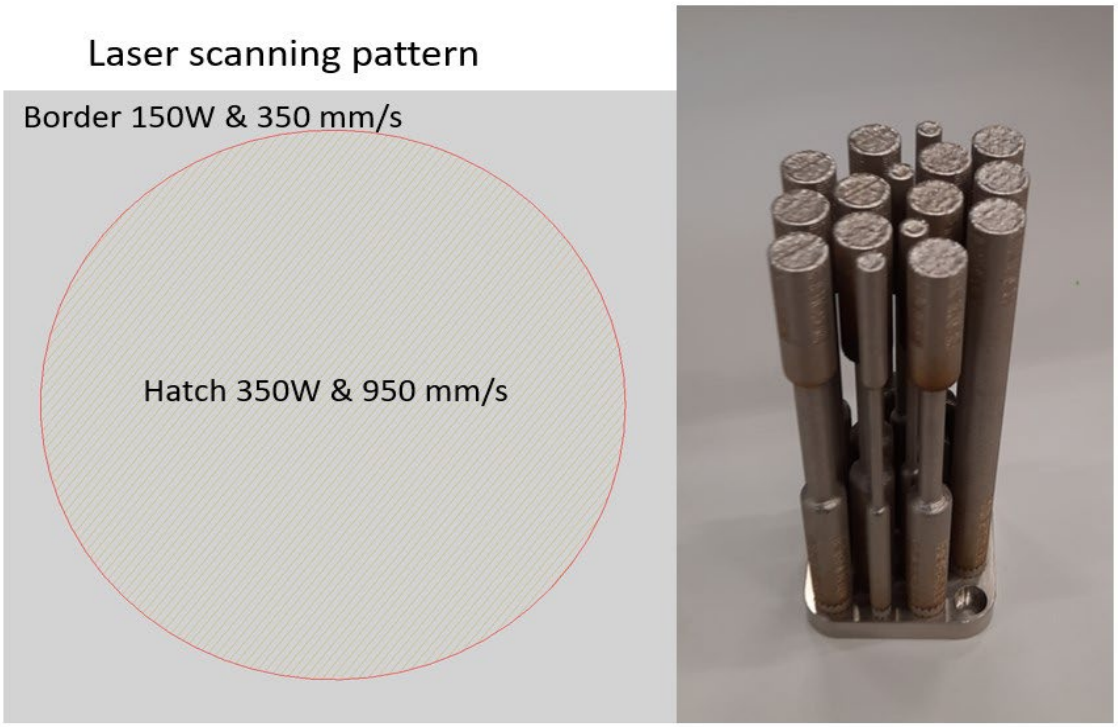

Figure 2. Laser scanning pattern in the gauge part and samples on a build plate.

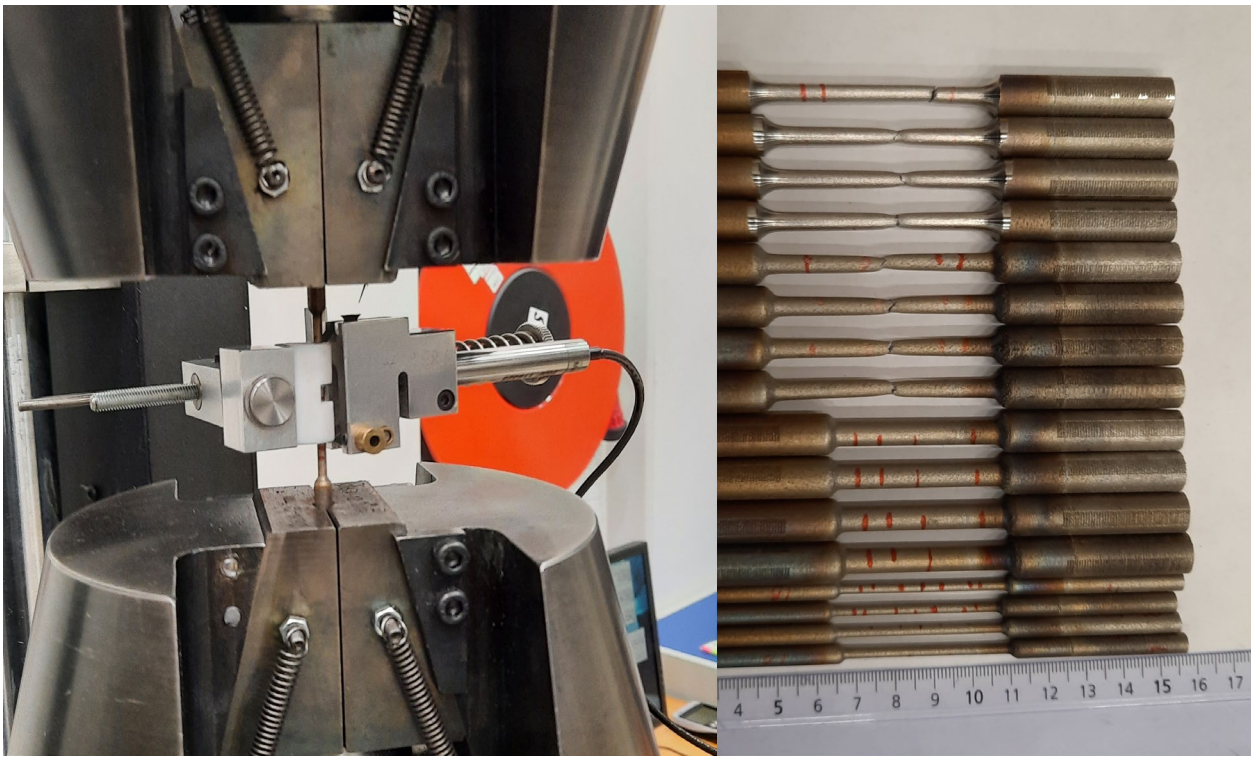

Figure 3. Sample with an extensometer attached and marked samples during testing.

Fig. 3 displays images of samples before and after testing, with visible markings applied for measuring %EL. In the figure, 5 mm diameter net-shape and machined samples have already been tested, while 2.5 mm and 6.0 mm samples are awaiting testing. It's important to note that the matte surface in the gauge part of machined samples is a result of plastic deformation (orange peel effect), while the original blank machined surface is visible at the transition from the gauge part to the grip part of the samples. To quantify the surface roughness, measurements were taken using a Mitutoyo SJ-210 machine. The surface roughness parameters for printed surfaces were measured to be Rz≈38.4 μm and Ra≈6.4 μm. Unfortunately, the machined gauge section of the sample could not be accessed by the Mitutoyo SJ-210 probe. Still, conservative estimates of roughness parameters, based on measurements of a cylinder machined by the same lathe machine, were Rz≈4.1 μm and Ra≈1.1 μm.

Results

Table1. Strength and ductility parameters summary.

Sample series	Machined samples	Net-shape d=6.0 mm	Net-shape d=5.0 mm	Net-shape d=2.5 mm
Yield Strength (YS) [MPa]	511	458	464	445
YS SD [MPa]	7	6	3	19
Tensile Strength (TS)	636	606	601	587
TS SD [MPa]	2	2	3	6
Elongation at fracture (%EL)	61.9	62.2	62.7	64.5
%EL SD	0.5	0.4	2.7	7.8
Area Reduction (%RA)	68.9	59.3	61.2	55.3
%RA SD	3.0	2.8	2.6	3.9

The results of the strength and ductility measurements are summarized in Table 1. The material does not display yield plateau; therefore, the yield strength was determined at 0.2% permanent elongation based on the extensometer data. The strength parameters reported in the Table 1 were determined using the nominal cross-section diameter i.e. the diameter specified in printing parameters for net-shape samples. Elongation at fracture %EL was determined over the length $l_0=5d_0$. Fig. 4 compares engineering stress-strain curves from one representative sample from each series. Table 1 also includes standard deviation (SD) in order to quantify the level of the scatter in the measurements, while Fig. 5 provides a visual illustration of the scatter by comparing engineering stress-strain curves from samples of the same series. Engineering stress-strain curves in Fig. 4 and Fig. 5 were constructed based on force and crosshead displacement data, with nominal sample diameters used for calculating engineering stress and a parallel length of 35.0 mm used for calculating engineering strain.

If we try to explain the difference in tensile strength between machined and net-shape samples of the same diameter by the reduction of initial cross section area as done by Salzbrenner et al. [11], a simple calculation shows that for the tensile strength to be equal, the actual load bearing area of net-shape sample would need to be:

$$A_{corrected\ net\ shape} = \frac{TS_{net\ shape}}{TS_{machined}} A_{machined} = \frac{601\ MPa}{636\ MPa} A_{machined} = 0.945\ A_{machined}$$

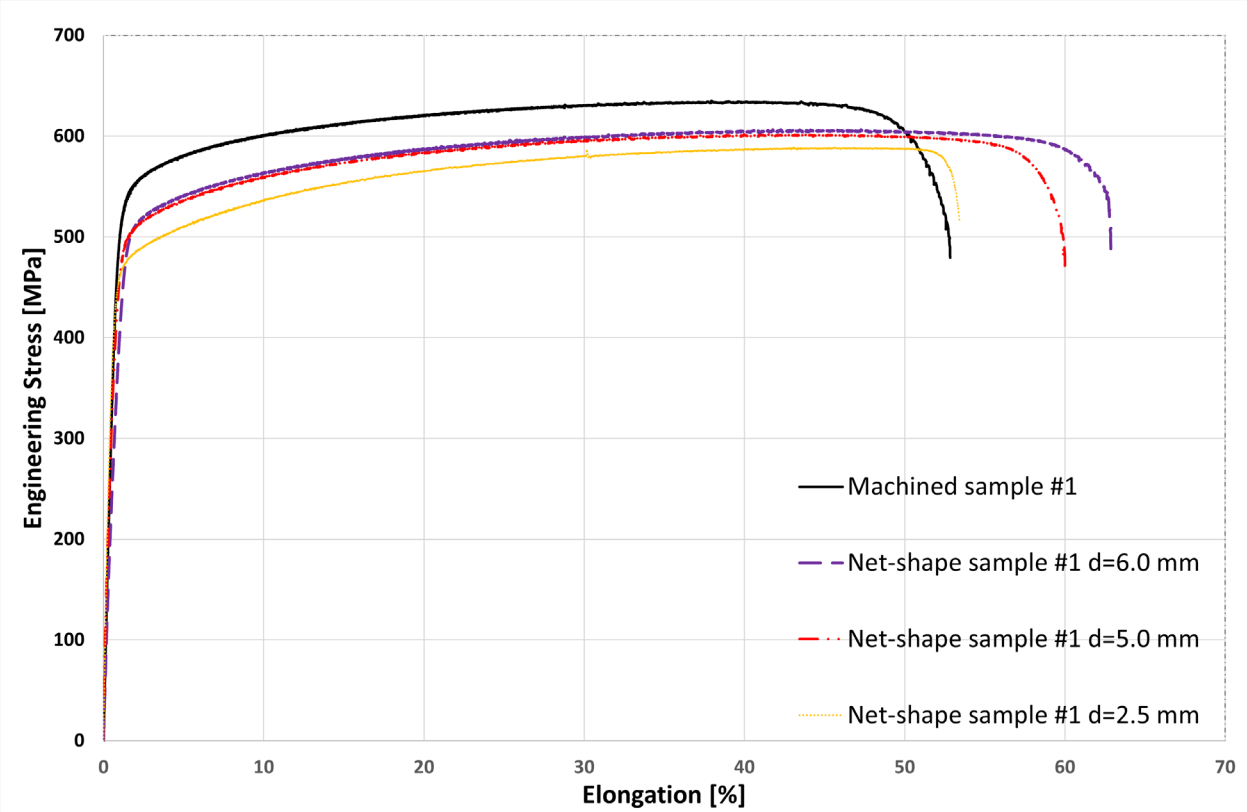

Figure 4 Representative engineering stress-strain curves for each series.

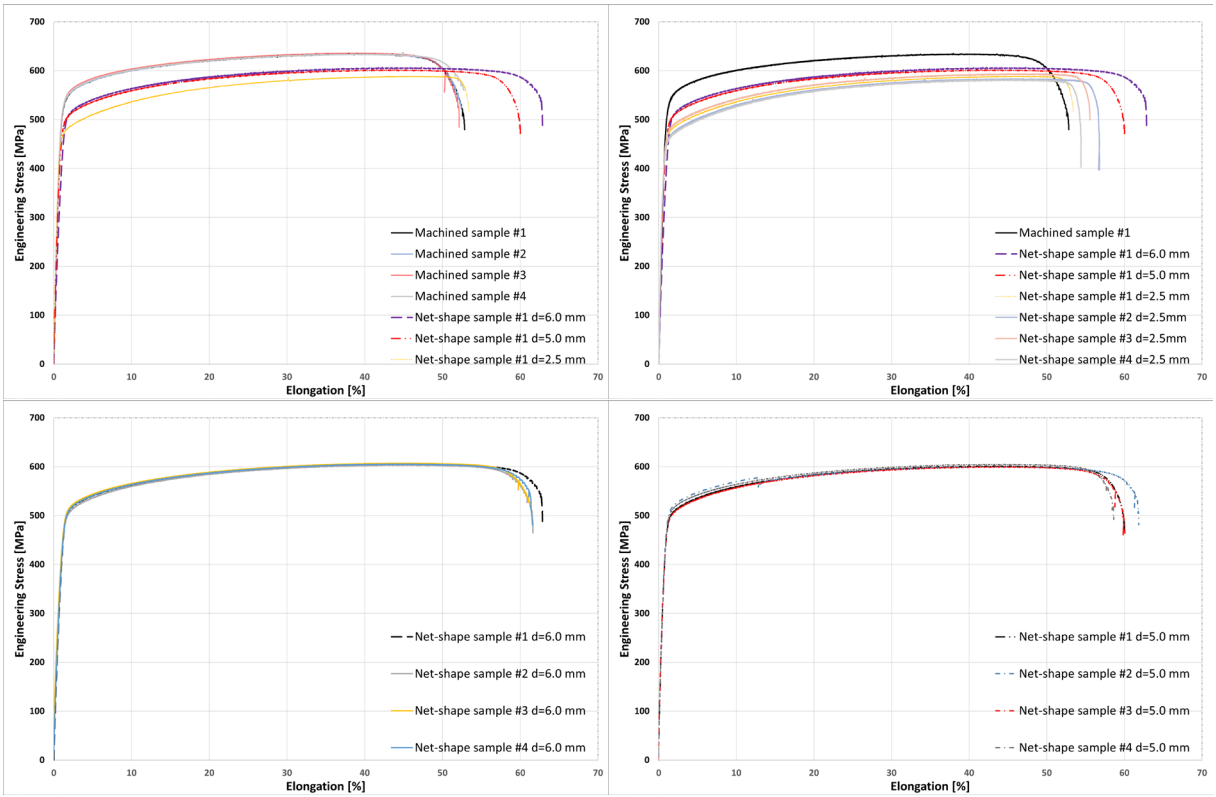

Figure 5 Illustration of scatter levels in different sample series.

resulting in an effective sample diameter

$$d_{corrected\ net\ shape} = \sqrt{0.945}\, d_0 = 0.972\, d_0 = 4.86 \text{ mm}$$

This would require peak surface roughness to be Rz≈(5-4.86) mm/2= 0.070 mm=70 μm which is nearly twice the measured value of Rz≈38.4 μm. If we would try to achieve same yield strength instead of same tensile strength, the required value of roughness would be even greater. This indicates that the surface roughness is likely not the only cause of difference in strength.

Discussions

Table 2 presents a summary of the literature finding with regard to effect of cross-section size on the strength of SLM-produced 316L steel and compares our findings with the results in the literature. It can be seen from Table 2 that, in the majority of cases, smaller diameter samples display lower strength than the larger diameter ones, making the findings of Yu et al. [4], [5] an anomaly. Our study is the only one that offers direct comparison between machined and net shape samples of the same diameter. As shown in the results section, the difference is unlikely to be explained purely by reduction of cross section area due to surface roughness and a second contributing factor must be that surface layer is to some degree weaker than the core of the sample e.g. contains more defects or has a different microstructure or texture. In the results presented in Table 2, only Yu et al.[5] explicitly discuss surface layer having different mechanical properties than the core of the cross section, but in their case surface layer appears to be stronger, not weaker. Microhardness plots of Wang et al. [7] indicate some lower hardness for near the surface for 1 mm and 2 mm struts, but no such effect is visible for 3 mm and 5 mm struts, however, average value of hardness increases with the strut diameter.

If we have a look at size effect in other common SLM-produced materials we find that in case of Ti-6Al-4V alloy, results in the literature are also conflicting Barba et al. [12] observed systematic increase in strength and decrease in ductility as the printed cross section is reduced while Dzugan et al [13] observed the opposite tendency i.e. lower strength in smaller thickness samples and larger strength in thicker samples. Despite reporting opposite effect of cross-section size on strength both [12] and [13] report that the size effect nearly disappears, when tensile samples are machined i.e. when the surface layer is removed. In case of AlSi10Mg another popular L-PBF alloy, only studies reporting reduction of strength for smaller diameters [14], [15] and reduction of hardness for smaller thicknesses [16] were found.

Conclusion

This study was motivated by the need to acquire fist hand data on size effect in SLM-produced steel, as the literature results are contradictory (see Table 2) and the mechanical properties of SLM-produced metals are strongly affected by the process parameters [17]. Our experimental results along with the literature review leave us to conclude that reduction of strength for smaller diameter samples is a more common tendency for SLM-produced 316L steel, while the strengthening effect observed by Yu et al. [5] is a peculiarity yet to be reproduced by other researchers. The observed reduction of strength is likely to be attributed to surface roughness and defects in the surface area as smaller diameter samples have a larger surface to area ratio in comparison with larger diameter samples. In case of tested 316L steel, this conclusion is also supported by machined samples displaying higher strength that net-shape samples of the same diameter.

Table2: Summary of literature findings on size effect in produced 316L steel

Study, laser power and scanning speed	Sample diameter/thickness range	Results	Explanation
Bültmann et al. [6] 195 W laser power combined with 900mm/s scanning speed	0.25 mm-0.7 mm plus "standard" machined samples of unreported geometry presumably 5.0 mm in diameter	Nearly constant strength with size. Machined samples were stronger than the struts samples	Multiple, but the reduction of strength due to "surface defects" seems to be the main reason
Wang et al. [7] Max laser power 200 W no further details reported.	0.25 mm to 5.0 mm diameter for microhardness 0.25 mm to 2.0 mm for tensile testing	Smaller diameter samples display lower strength. Average microhardness increases with strut diameter. No comparison with machined samples	The difference is attributed to different texture in different strut diameters
Roach et al. [8] Nominal laser power 103 W and scanning speed of 1400 mm/s	0.4 mm to 6.25 mm square cross-section sample	Smaller cross-section samples display lower strength. No comparison with machined samples	The difference is attributed to the influence of surface roughness
Yu et al. [4], [5] 150W laser power combined with 350 mm/s scan speed for both contour and hatching.	0.75 mm to 6.0 mm thickness samples	Smaller diameter samples display higher strength. No comparison with machined samples	The strengthening effect is explained by the formation of finer grains in the surface layer.
This study 150 W laser power combined with 350 mm/s for border/contour and 350 W combined with 950 mm/s for hatching.	2.5 mm, to 6.0 mm diameter net shape and 5.0 mm diameter machined samples	Smaller diameter samples display lower strength. Machined samples were stronger than unmachined ones	Presumably surface roughness and defects in the surface layer

* Recommended standard diameters for cylindrical samples are 5 mm, 10 mm, 14 mm and 20 mm [10]. It is reasonable to assume that the lowest diameter was used.

References

[1] N.-E. I. 52900, Additiv produksjon. Generelle prinsipper. Terminologi = Additive manufacturing. General principles. Terminology, vol. NS-EN ISO/. in Norsk Standard, vol. NS-EN ISO/. Lysaker: Norsk Standard, 2017.

[2] I. Jeon, L. Yang, K. Ryu, and H. Sohn, "Online melt pool depth estimation during directed energy deposition using coaxial infrared camera, laser line scanner, and artificial neural network," *Addit Manuf*, vol. 47, p. 102295, Nov. 2021. https://doi.org/10.1016/J.ADDMA.2021.102295

[3] B. Cheng, J. Lydon, K. Cooper, V. Cole, P. Northrop, and K. Chou, "Melt pool sensing and size analysis in laser powder-bed metal additive manufacturing," *J Manuf Process*, vol. 32, pp. 744–753, Apr. 2018. https://doi.org/10.1016/j.jmapro.2018.04.002

[4] J. Yu, D. Kim, K. Ha, J. B. Jeon, and W. Lee, "Strong feature size dependence of tensile properties and its microstructural origin in selectively laser melted 316L stainless steel," *Mater Lett*, vol. 275, p. 128161, Sep. 2020. https://doi.org/10.1016/J.MATLET.2020.128161

[5] J. Yu, D. Kim, K. Ha, J. B. Jeon, D. J. Kim, and W. Lee, "Size effect due to contour laser scanning in 316L stainless steel produced by laser powder bed fusion," *Journal of Materials Research and Technology*, vol. 15, pp. 5554–5568, Nov. 2021. https://doi.org/10.1016/J.JMRT.2021.11.034

[6] J. Bültmann, S. Merkt, C. Hammer, C. Hinke, and U. Prahl, "Scalability of the mechanical properties of selective laser melting produced micro-struts," *J Laser Appl*, vol. 27, p. null, 2015. https://doi.org/10.2351/1.4906392

[7] X. Wang, J. A. Muñiz-Lerma, O. Sanchez-Mata, M. A. Shandiz, and M. Brochu, "Microstructure and mechanical properties of stainless steel 316L vertical struts manufactured by laser powder bed fusion process," *Materials Science and Engineering: A*, vol. null, p. null, 2018. https://doi.org/10.1016/J.MSEA.2018.08.069

[8] A. M. Roach, B. C. White, A. Garland, B. H. Jared, J. D. Carroll, and B. L. Boyce, "Size-dependent stochastic tensile properties in additively manufactured 316L stainless steel," *Addit Manuf*, vol. 32, p. 101090, Mar. 2020. https://doi.org/10.1016/J.ADDMA.2020.101090

[9] L. Hitzler, J. Hirsch, B. Heine, M. Merkel, W. Hall, and A. Öchsner, "On the anisotropic mechanical properties of selective laser-melted stainless steel," *Materials*, vol. 10, no. 10, 2017. https://doi.org/10.3390/ma10101136

[10] ISO 6892-1:2019(en) Metallic materials — Tensile testing — Part 1: Method of test at room temperature. 2019. Accessed: Nov. 19, 2021. [Online]. Available: https://www.iso.org/standard/61856.html

[11] B. C. Salzbrenner *et al.*, "High-throughput stochastic tensile performance of additively manufactured stainless steel," *J Mater Process Technol*, vol. 241, pp. 1–12, Mar. 2017. https://doi.org/10.1016/j.jmatprotec.2016.10.023

[12] D. Barba, C. Alabort, Y. T. Tang, M. J. Viscasillas, R. C. Reed, and E. Alabort, "On the size and orientation effect in additive manufactured Ti-6Al-4V," *Mater Des*, vol. 186, p. 108235, Jan. 2020. https://doi.org/10.1016/J.MATDES.2019.108235

[13] J. Dzugan *et al.*, "Effects of thickness and orientation on the small scale fracture behaviour of additively manufactured Ti-6Al-4V," *Mater Charact*, vol. 143, pp. 94–109, Sep. 2018. https://doi.org/10.1016/J.MATCHAR.2018.04.003

[14] Z. Dong, X. Zhang, W. Shi, H. Zhou, H. Lei, and J. Liang, "Study of Size Effect on Microstructure and Mechanical Properties of AlSi10Mg Samples Made by Selective Laser Melting," *Materials 2018, Vol. 11, Page 2463*, vol. 11, no. 12, p. 2463, Dec. 2018. https://doi.org/10.3390/MA11122463

[15] D. Vysochinskiy and N. Akhtar, "On the Influence of Cross-Section Size on Measured Strength of SLM-Produced AlSi10Mg-Alloy," *Key Eng Mater*, vol. 926, pp. 132–140, Jul. 2022. https://doi.org/10.4028/P-G078SC

[16] N. Takata, H. Kodaira, A. Suzuki, and M. Kobashi, "Size dependence of microstructure of AlSi10Mg alloy fabricated by selective laser melting," *Mater Charact*, vol. 143, pp. 18–26, Sep. 2018. https://doi.org/10.1016/J.MATCHAR.2017.11.052

[17] A. Röttger *et al.*, "Microstructure and mechanical properties of 316L austenitic stainless steel processed by different SLM devices," *The International Journal of Advanced Manufacturing Technology 2020 108:3*, vol. 108, no. 3, pp. 769–783, Jul. 2020. https://doi.org/10.1007/S00170-020-05371-1